On the Local Delay and Energy Efficiency of HetNets with User Mobility

Xiaojie Dong†, Fu-Chun Zheng†, Ruixue Liu†, Xu Zhu*
† School of Electronic and Information Engineering
Harbin Institute of Technology (Shenzhen), Shenzhen, China
* Department of Electrical Engineering and Electronics, University of Liverpool, Liverpool, UK
Emails: {dongxiaojie, liuruixue}@stu.hit.edu.cn, {fzheng, xuzhu}@ieee.org

***Abstract*—With the development of fifth generation (5G) communications systems, heterogeneous networks (HetNets) have become a research hotspot. However, most of the existing work assumes that the user is static in HetNets. This hypothesis can greatly simplify system models, nevertheless it is not always accurate enough, because the user mobility has a significant effect on the performances of HetNets. Therefore, this paper studies the influence of the infinite user mobility in HetNets by using tools from stochastic geometry. The local delay and energy efficiency of HetNets based on Poisson point process (PPP) and Poisson cluster process (PCP) respectively are derived, the latter being more accurate to model the hot spot areas than the former. It was found that user mobility can reduce obviously the local delay and improve the energy efficiency under the high SIR regime. Moreover, the local delay is larger and the energy efficiency is lower under PCP than under PPP for infinite user mobility. In addition, the user mobility can reduce the function of the discontinuous transmission (DTX) scheme, which is used to improve the energy efficiency. Finally, the simulation results verify the accuracy of the numerical analyses.**

***Index Terms*—Heterogeneous networks (HetNets), local delay, energy efficiency, user mobility, Poisson point process (PPP), Poisson cluster process (PCP).**

I. Introduction

In recent years, due to the rapid increase of wireless communications traffic, ultra dense heterogeneous networks (HetNets) have become one of the most important technologies for the next generation mobile communications systems [1]. On the other hand, latency, energy efficiency (EE) and spectrum efficiency (SE) have been dedicated as three key performance indicators (KPIs) of the fifth generation (5G) communications systems. This paper will therefore study two of them for ultra dense HetNets: local delay and EE.

The latency as a KPI mainly consists of transmission delay and queuing delay. The transmission delay is termed the local delay in this paper, and is defined as the average time required to successfully transmit a packet on a wireless link. The local delay has been investigated for the static networks with Poisson point process (PPP) [2]– [4]. In reality, users can of course be very mobile. To this end, the local delay under infinite user mobility, where the users can move in the whole plane, was analyzed in [5] and [6] for ad hoc networks based on PPP. Other works have analyzed the effects and benefits of mobility on ad hoc network [7]– [8]. In addition, local delay of the clustered networks was studied in [9]. Moreover, in [11], the local delay was extended to the case of finite user mobility, where the users only move in a limited range rather than the whole plane. Nevertheless, little seems to have been reported on the local delay of HetNets based on PPP and PCP, with the latter being more accurate to model the hotspots than the former [12], [13] under user mobility.

The dramatic increase in communications traffic leads to the dense deployment of small cells in HetNets, which may increase greenhouse gas emission. Hence, the energy consumption of HetNets needs to be controlled, which demands that the network EE be investigated [14]– [16]. An analysis of EE has been carried out based on two-tier and three-tier HetNets [14]. In [15], analysis and optimization of EE under Coordinated Multipoint Transmission and Reception (CoMP) were investigated. Furthermore, tradeoff between EE and SE in 5G multi-operator networks with heterogeneous constraints was analyzed [16]. However, the EE of mobile HetNets with the discontinuous transmission (DTX) scheme, where the user is mobile, has not been investigated.

The contributions of this paper mainly include:

1) Using the Laplace transform of the aggregate interference, the local delay and EE of PPP and PCP distributions with DTX scheme under infinite user mobility have been derived. It is found that, for the infinite user mobility, the local delay under PPP is lower and the EE under PPP is higher than that of PCP.

2) We compared the static and the infinite mobility scenarios and found that the local delay under infinite mobility is lower and the EE is higher for high SIR threshold. Furthermore, the DTX scheme provides no benefit for HetNets with infinite user mobility, which implies that user mobility can reduce the function of the DTX scheme.

II. System Model

A. Heterogeneous Networks Model

We model a HetNet with K independent network tiers, and denote $\mathcal{K} = \{1, 2, ..., K\}$. Let Φ denote the set of overall BSs and Φ_i denote the set of BSs with the density denoted by λ_i in the ith tier. We therefore have $\Phi = \bigcup_{i \in \mathcal{K}} \Phi_i$. In addition, the

transmission power and the path-loss exponent are denoted by P_i and α_i for the ith-tier. Moreover, the transmission time is divided into discrete time slot, and a data packet is not counted as "transmitted" until the receiver can successfully decode. Furthermore, the typical mobile user now takes on infinite mobility, namely, the user is located at a different area in a different time slot. To simplify the model, we assume the user is located at origin in any time slot, but the locations of BSs are "redeployed" in each time slot [6]. Let $x_{i,j}$ denote the BS location in the ith tier, and $x_{k,0}$ denote the associated BS location. For the distribution of BS locations, this paper considers two models: PPP and PCP, with the latter being more realistic than the former. In addition, the DTX scheme with the mute probability of ζ [17], [18] is adopted at the BS, and the mute probability of BSs in the ith tier is denoted by ζ_i, namely, the BS in the ith tier stays active with probability of $1-\zeta_i$.

From the above network model, the aggregate interference of the typical user can be expressed by

$$I = \sum_{i\in\mathcal{K}} \sum_{x_{i,j}\in\Phi_i\setminus\{x_{k,0}\}} P_i h_{x_{i,j}} \|x_{i,j}\|^{-\alpha_i} \mathcal{T}(x_{i,j}\in\Phi_{i,t}) \quad (1)$$

where $\mathcal{T}(\cdot)$ is an indicator function, $\Phi_{i,t}$ denotes the active BS set in time slot t in the ith tier and $h_{x_{i,j}}$ denotes the power fading coefficient with the exponential distribution of unit mean (i.e., Rayleigh fading assumption). We consider that the power fading coefficient $h_{x_{i,j}}$ follows the same distribution in each time slot, therefore, $h_{x_{i,j}}$ is independent of the time slot t. Assuming that the kth-tier BS is associated with the user, the signal to interference ratio (SIR) can be calculated as

$$SIR = \frac{P_k h_{x_{k,0}} \|x_{k,0}\|^{-\alpha_k}}{I}, \quad (2)$$

assuming that the interference is large enough to neglect additive noise. We consider the average received signal strength (RSS) as an association criterion, and the index k of the associated BS can be expressed by

$$k = \arg\max_{i\in\mathcal{K}} P_i \|x_{i,0}\|^{-\alpha_i} \quad (3)$$

where $x_{i,0}$ is the nearest BS location in the ith tier.

In order to express a successful receive, we denote θ as the SIR threshold.

B. Laplace Transform

First, we consider the PPP as the distribution model of BSs. Let the distance between the associated BS and the typical user be reflected by r and denote $\mathcal{C}_k$ as the success event conditioned on the distance r. The successful transmission probability can be calculated as:

$$\begin{aligned} Pr(\mathcal{C}_k|r) &= (1-\zeta_k) Pr(SIR > \theta|r) \\ &= (1-\zeta_k) Pr(h_{x_{k,0}} > \frac{\theta I}{P_k r^{-\alpha_k}}|r) \\ &= (1-\zeta_k) E_I[exp(-\frac{\theta I}{P_k r^{-\alpha_k}})|r] \\ &= (1-\zeta_k) \mathcal{L}_I(\frac{\theta}{P_k r^{-\alpha_k}}|r). \end{aligned} \quad (4)$$

where $1-\zeta_k$ in (4) signifies that the associated BS stays active with the probability of $1-\zeta_k$. The conditional Laplace transform of the aggregate interference is given by

$$\begin{aligned} &{}_{PPP}\mathcal{L}_I(s|r) \\ &= \prod_{i=1}^{K} E\left[\prod_{x_{i,j}\in\Phi_i} exp(-sP_i h_{x_{i,j}} \|x_{i,j}\|^{-\alpha_i} \mathcal{T}(x_{i,j}\in\Phi_{i,t}))\right]. \end{aligned} \quad (5)$$

Using the conditional probability generating functional [20] of PPP, the Laplace transform of the aggregate interference is obtained by

$${}_{PPP}\mathcal{L}_I(s|r) = exp\left(-\sum_{i=1}^{K} \lambda_i \int_{R^2} [1-v_i(x)]dx\right) \quad (6)$$

where

$$v_i(x) = \frac{1-\zeta_i}{1+sP_i\|x\|^{-\alpha_i}} + \zeta_i. \quad (7)$$

The BSs in each tier now follow PCP, which consists of parent process and daughter process [20]. The density of parent points is denoted by $\lambda_{p,i}$ and the daughter points are uniformly located within a cluster, where the average number of daughter points follows Poisson process with mean $\bar{c}_i$ in the ith tier. Moreover, we consider the cluster structure as a circle with radius R_i in the ith tier.

The conditional Laplace transform of the aggregate interference is now given by

$$\begin{aligned} &{}_{PCP}\mathcal{L}_I(s|r) \\ &= \prod_{\substack{i=1\\ i\neq k}}^{K} E\left[\prod_{x_{i,j}\in\Phi_i} exp(-sP_i h_{x_{i,j}} \|x_{i,j}\|^{-\alpha_i} \mathcal{T}(x_{i,j}\in\Phi_{i,t}))\right]. \\ &E_x^{!}\left[\prod_{x_{k,j}\in\Phi_k} exp(-sP_k h_{x_{k,j}} \|x_{k,j}\|^{-\alpha_k} \mathcal{T}(x_{k,j}\in\Phi_{k,t}))\right] \end{aligned} \quad (8)$$

where $E_x^{!}[\cdot]$ is the reduced Palm expectation [20].

By using the conditional probability generating functional of PCP, the Laplace transform of the aggregate interference is obtained by

$$
\begin{aligned}
&{}_{PCP}\mathcal{L}_I(s|r) \\
&= exp\left(-\sum_{i=1}^{K}\lambda_{p,i}\int_{R^2}[1-exp(-\overline{c}_i\gamma_i(y))]dy\right) \\
&\times \int_{R^2} exp(-\overline{c}_k\gamma_k(y))f(y)dy
\end{aligned} \tag{9}
$$

where

$$
\gamma_i(y) = (1-\zeta_i)\int_{R^2}\frac{\|x-y\|^{-\alpha_i}}{\|x-y\|^{-\alpha_i}+1/sP_i}f(x)dx. \tag{10}
$$

The derivation is omitted here due to space.

C. Local Delay

As mentioned earlier, the local delay refers to the average number of time slots taken for a successful transmission in a wireless link [10]. Due to the infinite mobility, the probability of a successful transmission is same in each time slot, therefore, the local delay in a K-tier HetNet is

$$
D = \frac{1}{\sum_{k\in\mathcal{K}}\mathcal{A}_k E_r\left[Pr(\mathcal{C}_k|r)\right]} \tag{11}
$$

where $\mathcal{A}_k$ is the probability that the typical user is associated with the BS in the kth tier.

Here, the probability density function [5] of the distance r is expressed by

$$
f(r) = \frac{2\pi\lambda_k(1-\zeta_k)}{\mathcal{A}_k}exp(-\pi\sum_{i=1}^{K}\lambda_i(1-\zeta_i)(\frac{P_i}{P_k})^{\frac{2}{\alpha_i}}r^{\frac{2\alpha_k}{\alpha_i}}). \tag{12}
$$

First, using PPP to model the location of BSs, the local delay D_{PPP} based on the definition in (11) is given by

$$
\begin{aligned}
\frac{1}{D_{PPP}} = &\sum_{k=1}^{K}2\pi\lambda_k(1-\zeta_k)^2\int_0^{\infty}exp\left(-\pi\sum_{i=1}^{K}\lambda_i\right. \\
&\left.(\frac{P_i}{P_k})^{\frac{2}{\alpha_i}}r^{\frac{2\alpha_k}{\alpha_i}}(1-\zeta_i+(1-\zeta_i)\mathcal{G}(\alpha_i,\theta))\right)rdr
\end{aligned} \tag{13}
$$

where $\mathcal{G}(\alpha_i,\theta) = \int_1^{\infty}\frac{\theta}{\theta+t^{\frac{\alpha_i}{2}}}dt$. The derivation is omitted here due to space.

Considering some special cases, i.e., the mute probability $\{\zeta_k\} = \zeta$ and the path-loss exponent $\{\alpha_k\} = \alpha$, the local delay can be simplified as

$$
D_{PPP} = \frac{1}{1-\zeta} + \frac{\mathcal{G}(\alpha,\theta)}{1-\zeta}. \tag{14}
$$

From (14), there is no phase transition of local delay when $\zeta \in (0,1)$, because the infinite local delay occurs only when $\zeta = 1$ under infinite user mobility for any SIR threshold θ. Intuitively, for finite user mobility, where the user moves only in a limited area in each time slot, the finite local delay also exists because the finite user mobility falls in between the static and the infinite mobility. Moreover, when $\theta \to 0$, the local delay becomes $D_{PPP} \to 1/(1-\zeta)$, implying that the local delay is one time slot at least for low SIR threshold. For comparison, the local delay under static [10] is given by

$$
D_{PPP_s} = \frac{1}{1-\zeta}\cdot\frac{1}{1-(1-\zeta)\mathcal{Z}(\zeta,\alpha,\theta)}. \tag{15}
$$

From (15), when $\theta \to 0$, we have $D_{PPP_s} = \frac{1}{1-\zeta}$, which is same as that of infinite mobility. The result implies that for low SIR threshold, the user mobility has little effects on the local delay. Moreover, we can observe that the local delay is a monotonically increasing function of the mute probability ζ in (14), hence the minimum local delay happens at $\zeta = 0$. While this is not the case for the static result in (15).

We now consider PCP as the model of BSs. Similarly, the local delay D_{PCP} is calculated by

$$
\begin{aligned}
\frac{1}{D_{PCP}} = &\sum_{k=1}^{K}2\pi\lambda_k(1-\zeta_k)^2\int_0^{\infty}exp\left(-\pi\sum_{i=1}^{K}\lambda_{p,i}\right. \\
&(\frac{P_i}{P_k})^{\frac{2}{\alpha_i}}r^{\frac{2\alpha_k}{\alpha_i}}(\overline{c}_i(1-\zeta_i)+\mathcal{H}(\overline{c}_i,\zeta_i,\alpha_i,\theta)) \\
&\left.-\frac{\overline{c}_k(1-\zeta_k)}{R_k^2}\mathcal{G}(\alpha_k,\theta)r^2\right)rdr
\end{aligned} \tag{16}
$$

where $\mathcal{H}(\overline{c}_i,\zeta_i,\alpha_i,\theta) = \int_1^{\infty}[1-exp(\frac{-\overline{c}_i(1-\zeta_i)\theta}{\theta+t^{\frac{\alpha_i}{2}}})]dt$. The derivation is omitted here due to space.

The local delay under PPP and PCP under infinite user mobility are therefore respectively given in (13) and (16), and then we can find the relation of them. Let the cluster radius $\{R_k\} \to \infty$, and then the local delay under PCP in (16) can be simplified as

$$
\begin{aligned}
\frac{1}{D_{PCP}} &= \sum_{k=1}^{K}2\pi\lambda_k(1-\zeta_k)^2\int_0^{\infty}exp\left(-\pi\sum_{i=1}^{K}\lambda_{p,i}\right. \\
&\left.(\frac{P_i}{P_k})^{\frac{2}{\alpha_i}}r^{\frac{2\alpha_k}{\alpha_i}}(\overline{c}_i(1-\zeta_i)+\mathcal{H}(\overline{c}_i,\zeta_i,\alpha_i,\theta))\right)rdr \\
&\leq \sum_{k=1}^{K}2\pi\lambda_k(1-\zeta_k)^2\int_0^{\infty}exp\left(-\pi\sum_{i=1}^{K}\lambda_i\right. \\
&\left.(\frac{P_i}{P_k})^{\frac{2}{\alpha_i}}r^{\frac{2\alpha_k}{\alpha_i}}(1-\zeta_i+(1-\zeta_i)\mathcal{G}(\alpha_i,\theta))\right)rdr \\
&= \frac{1}{D_{PPP}}
\end{aligned} \tag{17}
$$

where $\mathcal{H}(\overline{c}_i,\zeta_i,\alpha_i,\theta)$ is substituted by $\overline{c}_i(1-\zeta_i)\mathcal{G}(\alpha_i,\theta)$ due to $1-exp(-x) \leq x$, $\forall x \geq 0$.

From (17), it is clear that the local delay under PCP is larger than that under PPP in the case of infinite mobility. Also, the local delay under PCP can not be lower than that of PPP for any key system parameters.

D. Energy Efficiency

In this paper, the network energy efficiency is defined as the ratio of average area network throughput τ to average area power consumption P_{area}. Hence, the energy efficiency [10], with unit nats/J/Hz, is given by

$$\begin{aligned}\eta_{EE} &= \frac{\tau}{P_{area}} \\ &= \frac{D^{-1} log(1+\theta)\sum_{i=1}^{K}(1-\zeta_i)\lambda_i}{\sum_{i=1}^{K}\lambda_i[(1-\zeta_i)(P_{i,a}+\Delta_i P_i)+\zeta_i P_{i,m}]}\end{aligned} \tag{18}$$

where $P_{i,a}$ is the static power of BS in active, and $P_{i,m}$ is the static power of BS in mute in the ith tier. Δ_i is the slope of power consumption in the ith tier. Especially, for PCP, we have the density $\lambda_i = \lambda_{p,i}\bar{c}_i$.

For the same key system parameters, i.e., same mute probability, path-loss exponent and SIR threshold and so on, the energy efficiency depends on the local delay D. Thus, from (17), we can realize that the energy efficiency under PCP is lower than that of PPP. Using the local delay derived in (13) and (16), the energy efficiency under PPP and PCP can be analyzed from (18). Inspired by [10], we consider two extreme cases: $\theta \to 0$ and $\theta \to \infty$, and let $\{\zeta_k\} = \zeta$ and $\{\alpha_k\} = \alpha$.

When $\theta \to 0$ (i.e., the low SIR regime), the local delay $D_{PPP} \sim 1/(1-\zeta)$, and the energy efficiency can be expressed by

$$\eta_{EE} = \frac{(1-\zeta)^2 log(1+\theta)\sum_{i=1}^{K}\lambda_i}{\sum_{i=1}^{K}\lambda_i[(1-\zeta)(P_{i,a}+\Delta_i P_i)+\zeta P_{i,m}]} \tag{19}$$

which shows that the energy efficiency is an increasing function of θ. In addition, the derivative of the energy efficiency over ζ can be calculated as

$$\eta_{EE}^{'}(\zeta) \sim -a(1-\zeta)^2 - b(1-\zeta^2) \tag{20}$$

where $a = \sum_{i=1}^{K}\lambda_i(P_{i,a}+\Delta_i P_i)$ and $b = \sum_{i=1}^{K}\lambda_i P_{i,m}$. From (20), $\eta_{EE}^{'}(\zeta)$ is negative, therefore, the energy efficiency will decrease with increase of ζ.

For $\theta \to \infty$ (i.e., the high SIR regime), the local delay $D \sim \mathcal{G}(\alpha,\theta)/(1-\zeta)$, therefore, the energy efficiency is given by

$$\eta_{EE} = \frac{(1-\zeta)^2 log(1+\theta)\sum_{i=1}^{K}\lambda_i}{\mathcal{G}(\alpha,\theta)(a(1-\zeta)+b\zeta)} \tag{21}$$

where $\mathcal{G}(\alpha,\theta) = C(\alpha)\theta^{\frac{2}{\alpha}} - {}_2F_1(1,\frac{2}{\alpha};1+\frac{2}{\alpha};-\frac{1}{\theta})$.

In this case, ${}_2F_1(1,\frac{2}{\alpha};1+\frac{2}{\alpha};-\frac{1}{\theta}) \to 1$, and we have $\mathcal{G}(\alpha,\theta) \sim C(\alpha)\theta^{\frac{2}{\alpha}} - 1$ and $\mathcal{G}^{'}(\alpha,\theta) \sim \frac{2}{\alpha}C(\alpha)\theta^{\frac{2}{\alpha}-1}$. Therefore, the effect of the SIR threshold θ on the energy efficiency is obtained by

$$\eta_{EE}^{'}(\theta) \sim \frac{1}{1+\theta} - \frac{2}{\alpha\theta} log(1+\theta) \tag{22}$$

which is less than zero when $\theta \to \infty$ due to $log(1+\theta) > \theta/(1+\theta)$. Thus, the energy efficiency will decrease with increase of the SIR threshold.

When $\theta \to \infty$, the derivative of the energy efficiency with respect to the mute probability can be expressed by

$$\eta_{EE}^{'}(\zeta) \sim -a(1-\zeta)^2 - b(1-\zeta^2). \tag{23}$$

which is less than zero when the mute probability $0 < \zeta < 1$. In the case, the energy efficiency is a decreasing function with respect to the mute probability, which is contrary to the static scenario [10]. The result indicates that the impact of the DTX scheme on the energy efficiency is reduced when the user is moving.

Furthermore, when the SIR threshold $0 < \theta < \infty$, we have

$$\eta^{'}(\theta) \sim \frac{1+\mathcal{G}(\alpha,\theta)}{1+\theta} - \mathcal{G}^{'}(\alpha,\theta) log(1+\theta) \tag{24}$$

From (24), we can obtain that the optimal SIR threshold satisfies

$$\theta^* > \frac{\alpha-2}{2} \tag{25}$$

which results from $log(1+\theta) < \theta$, $C(\alpha)\theta^{\frac{2}{\alpha}} < \mathcal{G}(\alpha,\theta)+1$ and $\mathcal{G}^{'}(\alpha,\theta) < \frac{2}{\alpha}C(\alpha)\theta^{\frac{2}{\alpha}-1}$.

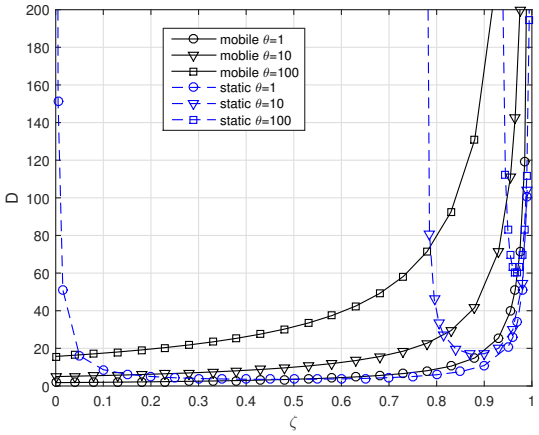

Fig. 1. Local delay D as a function of the mute probability ζ under PPP, where α=4.

III. Numerical Results

This section carries out some numerical analyses of the local delay and energy efficiency. A two-tier HetNet structure, consisting of macro cells (tier 1) and pico cells (tier 2), is used. For PCP, the deployment of macro cells is usually unicellular clustered, and therefore, $\bar{c}_1 = 1$. The other parameters are $P_1 = 20$W, $P_2 = 0.13$W, $P_{1,a} = 130$W, $P_{2,a} = 6.8$W, $\Delta_1 = 4.7$, and $\Delta_2 = 4.0$ [19].

In Fig. 1, local delay D as a function of the mute probability ζ under PPP is shown, where $\alpha = 4$. We can observe that

the local delay under infinite mobility spans a wider bands than that of static. And there is no network-contention phase transition of the local delay for any SIR threshold θ under infinite mobility. Therefore, the user mobility can change the properties of the local delay. The reason is that the correlation of the interference is reduced when the user is moving, leading to the obvious difference of the local delays between the static and infinite mobility for a high SIR threshold. Moreover, in the case of infinite mobility, the BSs are deployed at the density $\lambda_i(1-\zeta)$, implying that the impact of the DTX scheme is equivalent to the change in BS density. Generally, the user mobility is limited, therefore, the local delay under infinite mobility and static can respectively be regarded as two extreme cases of finite mobility.

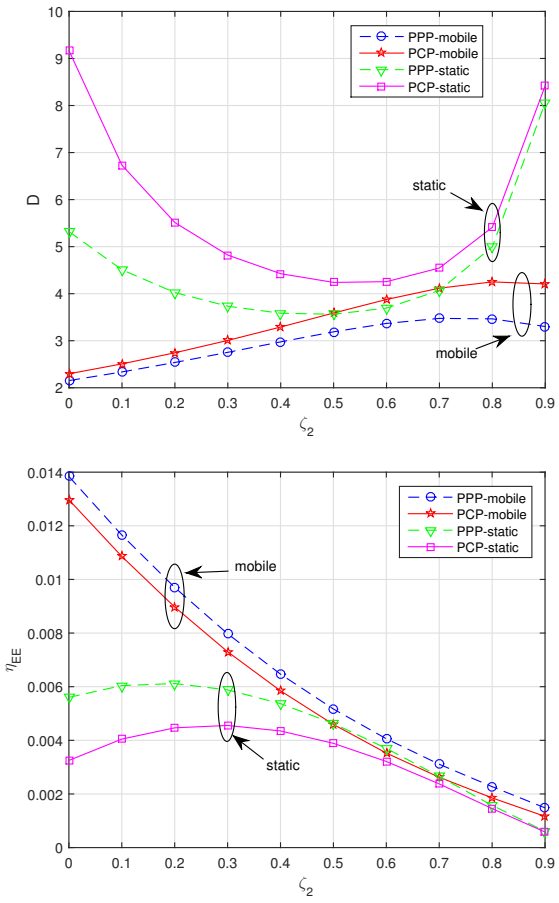

Fig. 2. Local delay and energy efficiency as a function of the mute probability ζ_2, where $\lambda_{p,1}$=1/(π500^2), $\lambda_{p,2}$=5/(π500^2), $\bar{c}_1$=1, $\bar{c}_2$=2, α=4, θ=1, R_1=800, R_2=500, $\zeta_1 = 0.4$.

In Fig. 2, local delay and energy efficiency as a function of the mute probability ζ_2 are shown, where $\lambda_{p,1} = 1/(\pi 500^2)$, $\lambda_{p,2} = 5/(\pi 500^2)$, $\bar{c}_1 = 1$, $\bar{c}_2 = 2$, $\alpha = 4$, $\theta = 1$, $R_1 = 800$, $R_2 = 500$, $\zeta_1 = 0.4$. No matter BSs are deployed on the basis of PCP or PPP, the local delay under infinite mobility is lower than that under static. Effected by the local delay, the energy efficiency under infinite mobility is higher than that under static. Furthermore, the local delay under the infinite mobility is a concave function of the mute probability ζ_2, whereas, the local delay under the static is a convex function of ζ_2. The reason is that the increasing of the associated distance is the dominating factor in the small ζ_2, however, the decreasing of the interference becomes the dominating factor in the large ζ_2, which is different from the static case.

In addition, the numerical results also show that the local delay under PCP is larger and the energy efficiency is lower than that of PPP for the static and the infinite mobility cases, which verifies the previous proof process in (17). The reason is that there is a large intra-cluster interference under PCP. Also, the results demonstrate that the mobility will not weaken the compact of the cluster under PCP. Moreover, we have found that the DTX scheme has no benefit to the energy efficiency in the infinite mobility case. As a result, the user mobility will reduce the contributions of DTX scheme on the local delay and energy efficiency.

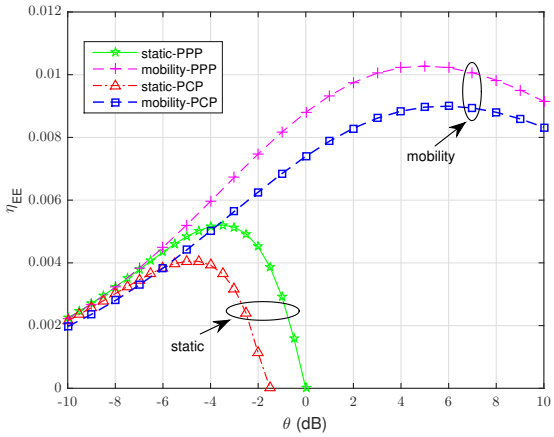

Fig. 3. Energy efficiency η_{EE} as a function of the SIR threshold θ, where λ_1=1/(π500^2), λ_2=10/(π500^2), α=3.5, $\zeta_1 = \zeta_2 = 0.2$, $\bar{c}_1 = 1$, $\bar{c}_2 = 5$, $R_1 = 600$, $R_2 = 800$.

Shown in Fig. 3 are energy efficiency η_{EE} as a function of the SIR threshold θ, where $\lambda_1 = 1/(\pi 500^2)$, $\lambda_2 = 10/(\pi 500^2)$, $\alpha = 3.5$, $\zeta_1 = \zeta_2 = 0.2$, $\bar{c}_1 = 1$, $\bar{c}_2 = 5$, $R_1 = 600$, $R_2 = 800$. The infinite mobility improves the energy efficiency, meanwhile, increases the optimal SIR threshold to maximum energy efficiency both of PPP and PCP. As a result, there are obvious differences between energy efficiencies under the static and the infinite mobility. Moreover, the optimal SIR threshold is larger than $(\alpha-2)/2$, which verifies our theoretical result in (25). Intuitively, the energy efficiency under the finite mobility is located between the static and the infinite mobility, and the optimal SIR

threshold θ_f^* under the finite mobility satisfies:

$$\theta_f^* > \sqrt{\frac{\alpha}{2}} - 1 \tag{26}$$

which results from the static case [10] and the optimal SIR threshold θ^* in (25) with a loose condition.

Fig. 4 shows local delay D as a function of the density of pico cells with different path-loss exponent, where $\lambda_1 = 1/(\pi 500^2)$, $\alpha_1 = 3.5$, $\zeta = 0$, $\theta = 1$. When $\alpha_1 > \alpha_2$, the local delay is a decreasing function of λ_2, when $\alpha_1 < \alpha_2$, however, the local delay is an increasing function of λ_2. If $\alpha_1 = \alpha_2$, the local delay is not related with density, which is consistent with (14). Therefore, the small path-loss exponent is bad for the dense deployment of pico cells, which largely increases the local delay. The reasons is the interference has a dominating effect on the local delay when $\alpha_2 < \alpha_1$, while, for $\alpha_1 > \alpha_2$, the shorter distance between the user and the associated BS has a primary effect on the local delay. When the path-loss exponent $\{\alpha_k\} = \alpha$, implying that the BSs have same channel environment, the impacts of the distance and the interference can be cancelled out in this case. In addition, in Fig. 4, we can observe that the analytical expressions match the simulation results with the tolerable gap.

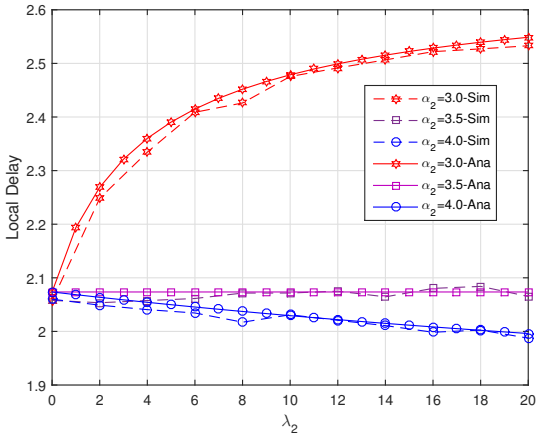

Fig. 4. Local delay D as a function of the density of Pico cells with different path-loss exponent, where λ_1=1/($\pi 500^2$), α_1=3.5, $\zeta = 0$, $\theta = 1$.

IV. Conclusion

In this paper, the local delay and energy efficiency of HetNets with infinite mobility based on PPP and PCP respectively have been derived. The numerical results revealed that the user mobility can change the properties of the local delay. In addition, the results theoretically demonstrated that the local delay and energy efficiency under infinite mobility are better than that of the static case, due to the weak correlation caused by user mobility. Meanwhile, we also found that the local delay is higher and the energy efficiency is lower under PCP than under PPP, which is due to the intra-cluster interference. Moreover, the user mobility can increase the optimal SIR threshold in terms of the energy efficiency, and the value range of the optimal SIR threshold was also obtained. Finally, the simulation results match the numerical results well.

V. Acknowledgements

This work was supported in part by the Science and Technology Innovation Commission of Shenzhen under Project No. JCYJ20170307151258279.

References

[1] M. Kamel and W. Hamouda and A. Youssef, "Ultra-Dense Networks: A Survey", *IEEE Commun. Surveys Tuts.*, vol, 18, no. 4, pp. 2522-2545, 2016.

[2] F. Baccelli and B. Blaszczyszyn, "A new phase transition for local delays in MANETs," in *Proc. IEEE INFOCOM*, 2010.

[3] Y. J. Chun, S. L. Cotton, M. O. Hasnay, and A. Ghrayeb, "Joint Optimization of Throughput and Delay Over PPP Interfered Relay Networks," in *Proc. IEEE PIMRC*, pp. 1-6, 2016.

[4] L. Liu, Y. Zhong, W. Zhang, and M. Haenggi, "On the Impact of Coordination on Local Delay and Energy Efficiency in Poisson Networks," *IEEE Wireless Commun. Lett.*, vol. 4, no. 3, pp. 241-244, Jun. 2015.

[5] M. Haenggi, "The Local Delay in Poisson Networks," *IEEE Trans. Inf. Theory*, vol. 59, no. 3, pp. 1788-1802, Mar. 2013.

[6] M. Haenggi, "Local delay in static and highly mobile Poisson networks with ALOHA," *IEEE Int. Conf. Commun.*, May. 2010.

[7] C. Bettstetter, "Mobility modeling in wireless networks: categorization, smooth movement, and border effects," in *Proc. IEEE MC2R*, vol. 5, no. 3, p. 66, 2001.

[8] Y. Peres, A. Sinclair, P. Sousi, and A. Stauffer, "Mobile geometric graphs: detection, coverage and percolation," in *Proc. IEEE SODA*, pp. 412-428, 2011.

[9] G. Alfano, R. Tresch, and M. Guillaud, "Spatial diversity impact on the local delay of homogeneous and clustered wireless networks," in *Proc. IEEE WSA*, pp. 1-6, 2011.

[10] W. Nie, Y. Zhong, F. Zheng, and W. Zhang, "HetNets With Random DTX Scheme: Local Delay and Energy Efficiency," *IEEE Trans. on Veh. Tech.*, vol. 65, no. 8, pp. 6601-6613, Aug. 2016.

[11] Z. Gong, and M. Haenggi, "The Local Delay in Mobile Poisson Networks," *IEEE Trans. Wireless Commun.*, vol. 12, no. 9, pp. 4766-4777, Sep. 2013.

[12] Y. J. Chun, M. O. Hasna, and A. Ghrayeb, "Modeling Heterogeneous Cellular Networks Interference Using Poisson Cluster Processes," *IEEE J. Sel. Areas Commun.*, vol. 33, no. 10, Oct. 2015.

[13] Y. Wang and Q. Zhu, "Modeling and Analysis of Small Cells Based on Clustered Stochastic Geometry," *IEEE Commun. Lett.*, vol. 21, no. 3, Mar. 2017.

[14] S. Rizvi, A. Aziz, M. T. Jilani, N. Armi, G. Muhammad and S. H. Butt, "An investigation of energy efficiency in 5G wireless networks," *IEEE ICCSS*, pp. 142-145, Jul. 2017.

[15] K. M. S. Huq, S. Mumtaz, J. Bachmatiuk, J. Rodriguez, X. Wang, and R. L. Aguiar, "Green HetNet CoMP: Energy Efficiency Analysis and Optimization," *IEEE Trans. Veh. Tech.*, vol. 64, no. 10, pp. 4670-4683. Oct. 2015.

[16] O. Aydin, E. A. Jorswieck, D. Aziz, and A. Zappone, "Energy-Spectral Efficiency Tradeoffs in 5G Multi-Operator Networks With Heterogeneous Constraints", *IEEE Trans. Wireless Commun.*, vol. 16, no. 9, pp. 5869-5881, Sep. 2017.

[17] P. Frenger, P. Moberg, J. Malmodin, Y. Jading, and I. Godor, "Reducing energy consumption in LTE with cell DTX," in *Proc. IEEE VTC Spring*, pp. 1-5, 2011.

[18] K. Hiltunen, "Utilizing eNodeB sleep mode to improve the energy efficiency of dense LTE networks," in *Proc. IEEE PIMRC*, pp. 3249-3253, 2013.

[19] G. Auer et al., "How much energy is needed to run a wireless network?" *IEEE Wireless Commun. Mag.*, vol. 18, no. 5, pp. 40-49, Oct. 2011.

[20] D. Stoyan, W. S. Kendall, and J. Mecke, *Stochastic Geometry and its Applications*, 2nd ed. Hoboken, NJ, USA: Wiley, 1996.